AEIC' 93

AL-AZHAR ENGINEERING THIRD
INTERNATIONAL CONFERENCE
December 18-21 1993

FACULTY OF ENGINEERING
AL - AZHAR UNIVERSITY
NASR CITY , CAIRO, EGYPT

VOLUME (5)
ELECTRICAL ENGINEERING
Electrical Power and Machines

AEIC'93

HAR ENGINEERING THIRD
NATIONAL CONFERENCE
BER 18-21, 1993

المؤتمر العلمي الدولي الثالث
كلية الهندسة - جامعة الازهر
من ٥ الى ٨ رجب ١٤١٤ هـ
من ١٨ الى ٢١ ديسمبر ١٩٩٣م

100	0.289	0.293	0.462	0.467
200	1.159	1.172	1.861	1.866
300	2.592	2.635	4.289	4.197
400	4.589	4.679	7.491	7.456
500	7.110	7.302	11.630	11.641
600	10.290	10.497	16.831	16.845
700	14.001	14.260	21.891	22.763
800	18.023	18.585	28.992	29.688
900	22.991	23.463	37.012	37.513
1000	27.856	28.884	45.961	46.226

A NEW BEARINGLESS TRAPIZOIDAL-PASSIVE-ROTOR SYNCHRONOUS MACHINE

S. M. Al-Kasimi*

* Assistant prof., Electrical and Computer Eng. Dept.,
Umm-Ul-Qura University, P.O.Box 6112, Makka, Saudi Arabia.

ABSTRACT

A bearingless machine is that which utilizes magnetic attraction between controlled electromagnets fixed to its stator and a laminated iron rotor, as shown in Fig.1. Fed from a chopper power amplifier that uses feedback signals, one electromagnet can support the rotor weight at constant airgap via field control.

The rotor under consideration, is constructed from laminated steel that is shaped to integral number of trapizoidal cycles as shown in Fig.2. Each of the torque-supplying drivers is a U-shaped magnet that acts as a two-pole machine in which each pole is split into two sub-poles. Each sub-pole is surrounded by a coil fed by an inverter such that the driver-field could be distorted among the four sub-poles. The rotor will move relative to the sub-poles to minimize reluctance, hence torque is obtained. The drivers are placed half-cycle apart to improve some of the torque properties.

This paper describes in theory the torque-characteristics of this bearingless machine that could be used for maintainance-free high-speed applications.

KEYWORDS

Trapizoidal; synchronous; bearingless; passive-rotor; machine; maglev; suspension.

INTRODUCTION

The Trapizoidal Linear Synchronous Motor, TLSM, is composed of two parts. The first: a magnet developed by McLean [1,2] and West [1,3]; is shown in Fig.3. The second: a trapizoidal rail developed by Al-Kasimi [4]; is shown in Fig.4.

The main poles of TLSM are excited by field current through dc coils, which is controlled to sustain a constant gap, Z. Each of the main poles is split into two sub-poles. These are surrounded by inverter-fed ac coils distorting the field among the sub-poles. whereby propulsion is obtained.

Al-Kasimi [5] has found that TLSM is a two-phase machine with coil connections as shown in magnet-A of Fig.5. This machine can give a maximum propulsive acceleration relative to gravity of $\sqrt{0.5}\,\pi\, Z/p$, where p is the pole-pitch shown in Fig.4.

The TLSM linear machine can be made rotary be winding its trapizoidal-rail circular as shown in Fig.2. This would require:

1. an integral number, N_P, of rail cycles within the rotor,
2. a separate controlled electromagnet to lift the rotor weight, and:
3. another TLSM to provide symmetrical drive. This suggests the configuration shown in Fig.1, where the twin TLSM drivers are placed horizontally opposite to each other; giving a Trapizoidal Rotary Synchronous Machine, TRSM.

This paper reviews TLSM machine relations to obtain the corresponding ones for TRSM drivers. These relations are for: sub-polar mmf excitations, energized areas, fluxes, flux-densities, pull forces, open circuit voltages, torque and coditions for maximum rating.

NOTATIONS

The symbols used in this paper are listed below:

- A sub-pole surface area
- A_i energized area of sub-pole i in driver-A
- B_i flux density over sub-pole i in driver-A
- D rotor diameter of TRSM
- E_i open circuit induced voltage at phase-i coil terminals in driver-A
- ϕ_k flux due to all sub-polar mmfs that leaves sub-pole k in driver-A
- F_v driver pull force against the rotor
- f rotor frequency of TRSM
- I_D current flowing in the field dc coils
- i_i current flowing in phase-i ac coils of driver-A
- μ_o permeability of air
- M_D net dc mmf excitation of field winding per pole
- $\overline{M}_D$ optimum M_D value for maximum torque
- m peak value of ac mmf excitation (
- $\overline{m}$ optimum m value for maximum t
- m_i ac mmf excitation of phase-i arm
- m_j resultant mmf excitation around
- N number of turns of ac coil arounc
- N_D number of turns of dc coil arounc
- N_P number of rail cycles within roto
- P driver steady pull force against t
- p pole-pitch
- θ phase angle of ac excitation of di
- $\overline{\theta}$ optimum phase angle at maximu
- T, T' time period to complete one cycl
- T_q TRSM torque
- T_{q_m} maximum TRSM torque
- t time starting zero when rail com
- u speed of rotor-rail relative to dri
- ω, ω' angular frequency in TLSM, TR
- Z energized air gap

ASSUMPTIONS

For simplicity, the following assumptions

1. All sub-poles have the same su them fed with sinusoidal ac cur
2. Width of slot in the main poles coils around them are constants
3. Rotor curvature, fringing, leaka and other drag forces are all ig
4. Air gap, Z, is homogeneous ov both at rail-surface and at mag of Z is ignored in comparision
5. The energized area per pole i belongs to one of the two adja assumed to vary sinusoidally b
6. The rotor, assumed rigid, has The frequency of rotation is al
7. The driver force is composed to rotational axis. Although s exerted, it will be ignored.
8. Flux linkage for any ac coil va when its sub-pole is fully uncou is fully coupled to rail.

FREQUENCY RELATIONS

When the rail of TLSM moves in the dir T, and switching angular frequency, ω, current are given respectively by:

$$T = 4p/u \;\&$$

s; passive-rotor; machine; maglev; suspension.

Motor, TLSM, is composed of two parts. The an [1,2] and West [1,3]; is shown in Fig.3. The by Al-Kasimi [4]; is shown in Fig.4.

ed by field current through dc coils, which is , Z. Each of the main poles is split into two inverter-fed ac coils distorting the field among obtained.

is a two-phase machine with coil connections as chine can give a maximum propulsive accelera- where p is the pole-pitch shown in Fig.4.

de rotary be winding its trapizoidal-rail circular :

cycles within the rotor,
magnet to lift the rotor weight, and:
mmetrical drive. This suggests the configura- he twin TLSM drivers are placed horizontally g a Trapizoidal Rotary Synchronous Machine,

elations to obtain the corresponding ones for sub-polar mmf excitations, energized ar- open circuit voltages, torque and coditions for

ted below:

driver-A
driver-A

t phase-i coil terminals in driver-A
that leaves sub-pole k in driver-A
otor

coils
oils of driver-A

winding per pole
torque

m peak value of ac mmf excitation of any phase per sub-pole
$\bar{m}$ optimum m value for maximum torque
m_i ac mmf excitation of phase-i armature winding per sub-pole
m_j resultant mmf excitation around sub-pole j of driver-A
N number of turns of ac coil around any sub-pole
N_D number of turns of dc coil around any pole
N_P of rail cycles within rotor
P driver steady pull force against the rotor
p pole-pitch
θ phase angle of ac excitation of driver-A
$\bar{\theta}$ optimum phase angle at maximum torque
T, T' time period to complete one cycle in TLSM, TRSM
T_q TRSM torque
$T_{\hat{q}}$ maximum TRSM torque
t time starting zero when rail completely links sub-poles 1 and 3 of driver-A
u speed of rotor-rail relative to driver
ω, ω' angular frequency in TLSM, TRSM
Z energized air gap

ASSUMPTIONS

For simplicity, the following assumptions were made in the analysis to come.

1. All sub-poles have the same surface area, A, with identical ac coils around them fed with sinusoidal ac current phase-locked to rotor-rail.
2. Width of slot in the main poles is negligible, and field mmf excitations of dc coils around them are constants.
3. Rotor curvature, fringing, leakages, steel and copper losses, windage, friction and other drag forces are all ignored.
4. Air gap, Z, is homogeneous over the sub-poles, with equal energized areas both at rail-surface and at magnet-pole-surface throughout motion. The size of Z is ignored in comparision with the rotor diameter, D.
5. The energized area per pole is composed of two portions. Each portion belongs to one of the two adjacent sub-poles within the main pole, and is assumed to vary sinusoidally between zero and A.
6. The rotor, assumed rigid, has fixed axis of rotation with no axial motion. The frequency of rotation is also assumed constant with time.
7. The driver force is composed of two components only in the plane normal to rotational axis. Although some force component along rotational axis is exerted, it will be ignored.
8. Flux linkage for any ac coil varies sinusoidally between a minimum of zero when its sub-pole is fully uncoupled to rail and a maximum when its sub-pole is fully coupled to rail.

FREQUENCY RELATIONS

When the rail of TLSM moves in the direction indicated in Fig.4, the switching period, T, and switching angular frequency, ω, of the two-phase inverter providing armature current are given respectively by:

$$T = 4p/u \;\&\; \qquad \omega = \pi u/2p\,.$$

For TRSM; T' and ω' are related to f and Np by:

$$T' = 1/f = T\,N_P \; \& \qquad \omega' = 2\pi\,f = \omega/N_P\,.$$

Hence, u and ω are substituted as:

$$u = 4p\,f\,N_P \; \& \qquad \omega = 2\pi\,f\,N_P\,.$$

The rotor diameter, D, is related to N_P as:

$$D = 4p\,N_P/\pi\,.$$

MAGNETIC SUB-POLAR EXCITATIONS

When the rail of TLSM moves in the direction indicated in Fig.4, Al-Kasimi [4,5] found that the flux linkages of ac coils per magnet vary in-phase for adjacent sub-poles and so can be series-connected forming one phase. This phase is in quadrature to the other phase of the opposing sub-poles. This illustrates the connections shown in Fig.5, per driver. Note that in each driver, phase-A leads phase-B by a quarter of a cycle; and that the dc coils are connected so as to build constructive flux components. Hence, with:

$$M_D = N_D\,I_D\,,$$

$$m_A(t) = N\,i_A(t) = m\,cos(\omega\,t+\theta) \; \& \qquad m_B(t) = N\,i_B(t) = m\,sin(\omega\,t+\theta);$$

and assuming positive sense when forcing flux to leave the sub-poles, then:

$$m_1(t) = -M_D - m_A(t)\,, \qquad m_2(t) = -M_D + m_A(t)\,,$$
$$m_3(t) = +M_D + m_B(t) \; \& \qquad m_4(t) = +M_D - m_B(t)\,.$$

These relations hold true for each TRSM driver.

ENERGIZED SUB-POLAR AREAS

For TLSM as well as TRSM, the energized areas are approximated to:

$$A_1(t) = (A/2)\,[1 + cos(\omega\,t + \pi/4)\,, \qquad A_2(t) = (A/2)\,[1 - cos(\omega\,t + \pi/4)]\,,$$
$$A_3(t) = (A/2)\,[1 + cos(\omega\,t - \pi/4)] \; \& \qquad A_4(t) = (A/2)\,[1 - cos(\omega\,t - \pi/4)]\,.$$

MAGNETIC SUB-POLAR FLUXES

For TLSM, the fluxes are given [5], using superposition, as:

$$\phi_1(t) = -\mu_0\,A_1\,[2\,M_D + 2\,m_A + m\,sin(2\,\omega\,t + \theta - \pi/4)]/2Z\,,$$
$$\phi_2(t) = -\mu_0\,A_2\,[2\,M_D - 2\,m_A + m\,sin(2\,\omega\,t + \theta - \pi/4)]/2Z\,,$$
$$\phi_3(t) = +\mu_0\,A_3\,[2\,M_D + 2\,m_B - m\,sin(2\,\omega\,t + \theta - \pi/4)]/2Z \; \&$$
$$\phi_4(t) = +\mu_0\,A_4\,[2\,M_D - 2\,m_B - m\,sin(2\,\omega\,t + \theta - \pi/4)]/2Z\,.$$

These relations hold true for each TRSM driver.

MAGNETIC SUB-POLAR FLUX-DEN

For both TLSM and TRSM, the above equati

$$B_1(t) = \phi_1(t)/A_1(t) = -\mu_0\,[2\,M_D + 2\,m$$
$$B_2(t) = \phi_2(t)/A_2(t) = -\mu_0\,[2\,M_D - 2\,m$$
$$B_3(t) = \phi_3(t)/A_3(t) = +\mu_0\,[2\,M_D + 2\,m$$
$$B_4(t) = \phi_4(t)/A_4(t) = +\mu_0\,[2\,M_D - 2\,m$$

DRIVER PULL FORCE

The TRSM pull force, F_{v_A}, of driver-A is de

$$F_{v_A}(t) = \mu_0\,A\,[8\,M_D^2 + 3\,m^2 + 8\,M_D\,m\,co$$

This is composed of two components:

1. one steady, and can be totally ca between driver-A and driver-B wa
2. one pulsating at four times the sy canceled by that of driver-B if, add driver-B was kept at an integral n

The time-shift is obtained by placing driver This is seen to give half-cycle time-shift for

On the other hand, the θ-shift is obtained driver-B to the two-phase inverter supply. Fig.5.

Hence, the driver-B pull force, F_{v_B}, is obt steady pull force, P, of either driver again

$$P = \mu_0\,A\,[8\,M_D^2 + 3\,m^2 + $$

OPEN CIRCUIT VOLTAGES

For TLSM and TRSM, the open cicuit motor in Fig.5 can be found to be:

$$E_A(t) = -\mu_0\,\omega\,A\,M_D$$
$$E_B(t) = -\mu_0\,\omega\,A\,M_D$$

TRSM TORQUE

The twin TRSM drivers produce opposite gives the machine torque, T_q, which can

$$T_q = (E_A\,i_A + E_B\,i_B)/(\pi\,f) = \mu$$

f and Np by:

$$P \;\&\quad \omega' = 2\pi f = \omega/N_P \,.$$

$$P \;\&\quad \omega = 2\pi f N_P \,.$$

N_P as:

$$= 4p\, N_P/\pi \,.$$

CITATIONS

ne direction indicated in Fig.4, Al-Kasimi [4,5]
oils per magnet vary in-phase for adjacent sub-
forming one phase. This phase is in quadrature
ub-poles. This illustrates the connections shown
n driver, phase-A leads phase-B by a quarter of a
cted so as to build constructive flux components.

$$I_D = N_D\, I_D \,,$$

$$) \;\&\quad m_B(t) = N\, i_B(t) = m\, sin(\omega t + \theta);$$

rcing flux to leave the sub-poles, then:

$$3 \,,\qquad m_2(t) = -M_D + m_A(t) \,,$$
$$) \;\&\quad m_4(t) = +M_D - m_B(t) \,.$$

RSM driver.

EAS

rgized areas are approximated to:

$$) \,,\qquad A_2(t) = (A/2)\,[1 - cos(\omega t + \pi/4)],$$
$$)] \;\&\quad A_4(t) = (A/2)\,[1 - cos(\omega t - \pi/4)].$$

IXES

using superposition, as:

$$m_A + m\, sin(2wt + \theta - \pi/4)]/2Z \,,$$
$$m_A + m\, sin(2wt + \beta - \pi/4)]/2Z \,,$$
$$m_B - m\, sin(2\omega t + \theta - \pi/4)]/2Z \;\&$$
$$m_B - m\, sin(2\omega t + \theta - \pi/4)]/2Z \,.$$

RSM driver.

MAGNETIC SUB-POLAR FLUX-DENSITIES

For both TLSM and TRSM, the above equations give the sub-polar flux densities as:

$$B_1(t) = \phi_1(t)/A_1(t) = -\mu_0\,[2\,M_D + 2\,m_A + m\, sin(2wt + \theta - \pi/4)]/2Z \,,$$
$$B_2(t) = \phi_2(t)/A_2(t) = -\mu_0\,[2\,M_D - 2\,m_A + m\, sin(2\omega t + \theta - \pi/4)]/2Z \,,$$
$$B_3(t) = \phi_3(t)/A_3(t) = +\mu_0\,(2M_D + 2\,m_B - m\, sin(2wt + \theta - \pi/4)]/2Z \;\&$$
$$B_4(t) = \phi_4(t)/A_4(t) = +\mu_0\,(2M_D - 2\,m_B - m\, sin(2\omega t + \theta - \pi/4)]/2Z \,.$$

DRIVER PULL FORCE

The TRSM pull force, F_{v_A}, of driver-A is deduced [5] as:

$$F_{v_A}(t) = \mu_0\, A\,[8\,M_D^2 + 3\,m^2 + 8\,M_D\, m\, cos(\theta - \pi/4) + m^2\, sin(4\omega t + 2\,\theta)]/8Z^2 \,.$$

This is composed of two components:

1. one steady, and can be totally canceled by that of driver-B if the θ-shift between driver-A and driver-B was zero; and:
2. one pulsating at four times the synchronous frequency, and can be totally canceled by that of driver-B if, additionally, the t-shift between driver-A and driver-B was kept at an integral number of quarter-rail-cycles.

The time-shift is obtained by placing driver-A opposite to driver-B as shown in Fig.1. This is seen to give half-cycle time-shift for driver-B.

On the other hand, the θ-shift is obtained by carefully connecting the two phases of driver-B to the two-phase inverter supply. This explaines the connections shown in Fig.5.

Hence, the driver-B pull force, F_{v_B}, is obtained as: $F_{v_B}(t) = F_{v_A}(t)$. This gives the steady pull force, P, of either driver against the rotor as:

$$P = \mu_0\, A\,[8\,M_D^2 + 3\,m^2 + 8\,M_D\, m\, cos(\theta - \pi/4)]/8Z^2 \,. \tag{1}$$

OPEN CIRCUIT VOLTAGES

For TLSM and TRSM, the open cicuit induced voltages at ac terminals of either motor in Fig.5 can be found to be:

$$E_A(t) = -\mu_0\, w\, A\, M_D\, N\, sin(\omega t + \pi/4)/Z \;\&$$
$$E_B(t) = -\mu_0\, w\, A\, M_D\, N\, sin(\omega t - \pi/4)/Z \,.$$

TRSM TORQUE

The twin TRSM drivers produce oppositely-directed equal driving forces. This couple gives the machine torque, T_q; which can be obtained using the energy principle as:

$$T_q = (E_A\, i_A + E_B\, i_B)/(\pi f) = \mu_0 \pi\, A\, D\, M_D\, m\, sin(\theta - \pi/4)/(2p\, Z) \,. \tag{2}$$

This is seen to be steady with $M_D(\theta, m)$ implicitly function of θ and m given in eq.(1) for any pull, P.

MAXIMUM TORQUE

The maximum of T_q for a given P and θ occures at $\overline{M}_D(\theta)$ and $\overline{m}(\theta)$. This could be found using eqs.(1) and (2) to give:

$$\overline{M}_D(\theta) = M_D(\theta, \overline{m}(\theta)) = \sqrt{0.375}\,\overline{m}(\theta)\,.$$

$$\overline{m}(\theta) = 2\,Z\,\sqrt{\frac{P}{\mu_0\,A\,[3+\sqrt{6}\,cos(\theta-\pi/4)]}}\ \&$$

$$T_q(\theta) = (\pi\,Z/p)\,.\,\frac{sin(\theta-\pi/4)}{\sqrt{6}+2\,cos(\theta-\pi/4)}\,.\,D\,P\,.$$

On the other hand; the maximum value, T_{q_x}, of $T_q(\theta)$ occures at $\overline{\theta}$, found as:

$$\overline{\theta} = 5\pi/4 \pm cos^{-1}\sqrt{(2/3)}\,.$$

This would give:

$$\overline{m} = 2\,Z\,\sqrt{P/(\mu_0\,A)}\ \&$$

$$T_{q_x} = \mid T_q(\overline{\theta})\mid = \sqrt{0.5}\,D\,P\,(\pi\,Z/p)\,.$$

CONCLUSION

The TRSM bearingless-machine can produce, at any given rotational speed, a maximum torque of: $\sqrt{0.5}\,\pi\,Z\,/p$ relative to its pull-diameter product.

REFERENCES

[1] McLean, G. W. and West, A. N. (1984). Combined Lift and Thrust for Maglev Vehicles Using the Zigzag Synchronous Motor. Proc. Int. Conf. on Maglev Transport Now and for the Future, IMechE: 87-97.

[2] McLean, G. W. (1988). Review of Recent Progress in Linear Motors. IEE Proc., Vol. 35, Part B, No. 6: 380-416.

[3] West, A. N. (1982). The Control of a Linear Homopolar Synchronous Machine. PhD Thesis, Elect. Eng. Dept., Manchester University.

[4] Al-Kasimi, S. M. (1992). A New Synchronous Motor for Maglev Train With Integrated Lift and Thrust Using A Trapizoidal Rail. Proc. Second Middle East Power System Conf., MEPCON'92, Assiut University, Egypt: 67-69.

[5] Al-Kasimi, S. M. and BaQubas, A. O. (1991). The Acceleration Characteristics of The Trapizoidally Railed Linear Homopolar Synchronous Motor as Compared to The Zigzag Version for Maglev Applications. Proc. Azhar Engineering Second International Conference, AEC'91, Al-Azhar University, Egypt, Vol. 5: 392-409.

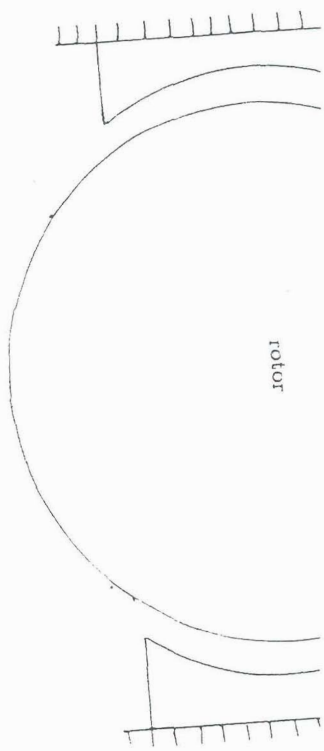

Fig.1 Section view of bearingless machine

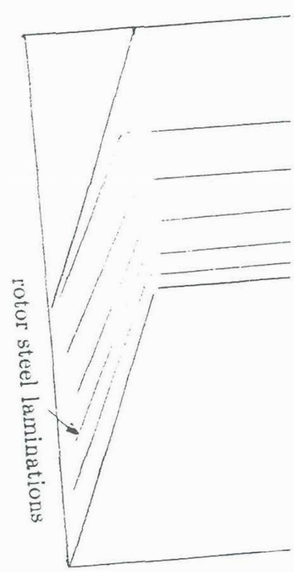

Fig.2 Front view of TRSM rotor

itly function of θ and m given in eq.(1)

es at $\overline{M}_D(\theta)$ and $\overline{m}(\theta)$. This could be

$$\overline{0.375}\ \overline{m}(\theta)\,,$$

$$\frac{P}{\overline{6}\,cos(\theta - \pi/4)]}\ \&$$

$$\frac{\theta - \pi/4)}{\cos(\theta - \pi/4)}\,.\,D\,P\,.$$

of $T_q(\theta)$ occures at $\overline{\theta}$, found as:

$$\sqrt{(2/3)}\,.$$

&

$$D\,P\,(\pi\,Z/p)\,.$$

at any given rotational speed, a maxi-
l-diameter product.

). Combined Lift and Thrust for Ma-
ous Motor. Proc. Int. Conf. on Maglev
IE: 87-97.

; Progress in Linear Motors. IEE Proc.,

near Homopolar Synchronous Machine.
er University.

ronous Motor for Maglev Train With
izoidal Rail. Proc. Second Middle East
t University, Egypt: 67-69.

991). The Acceleration Characteristics
polar Synchronous Motor as Compared
tions. Proc. Azhar Engineering Second
har University, Egypt, Vol. 5: 392-409.

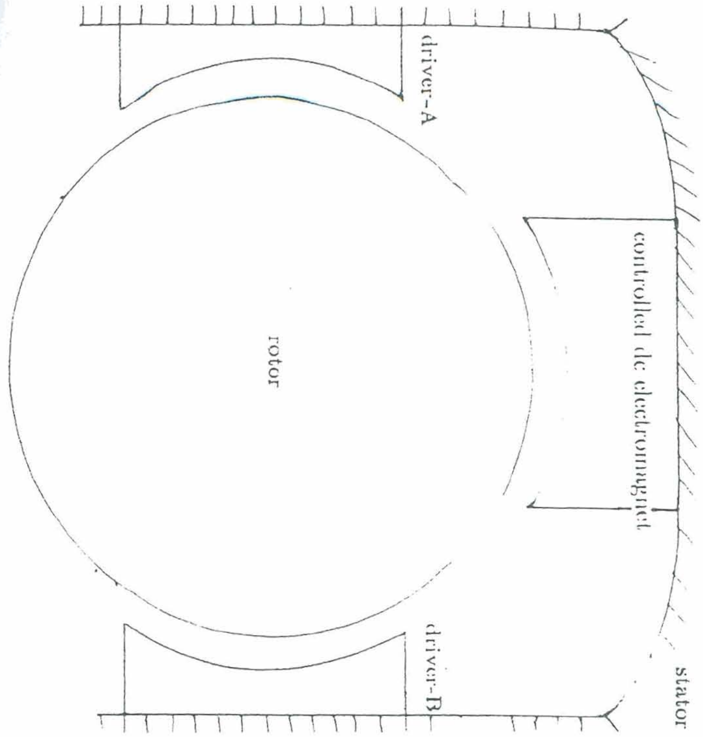

Fig.1 Section view of bearingless machine

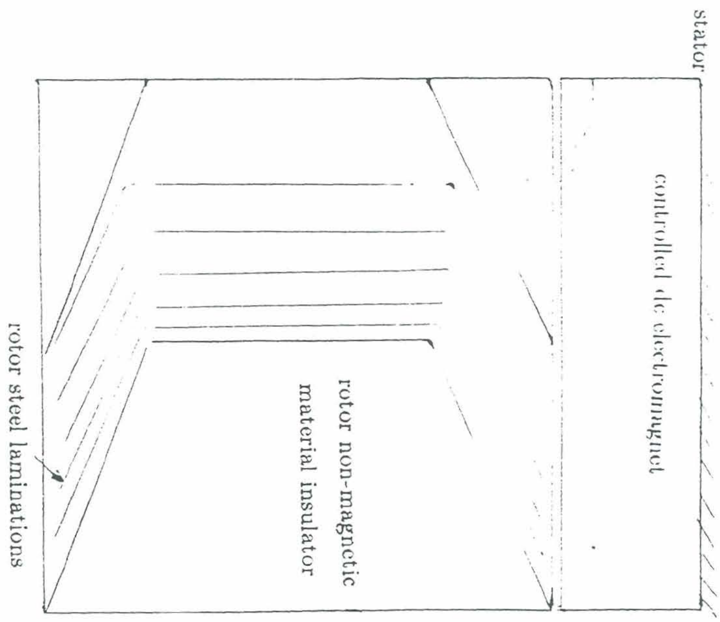

Fig.2 Front view of TRSM rotor

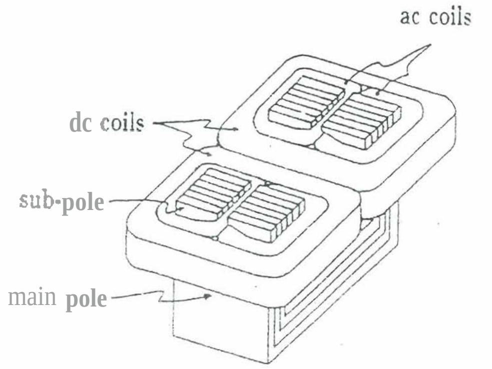

Fig.3 Magnet

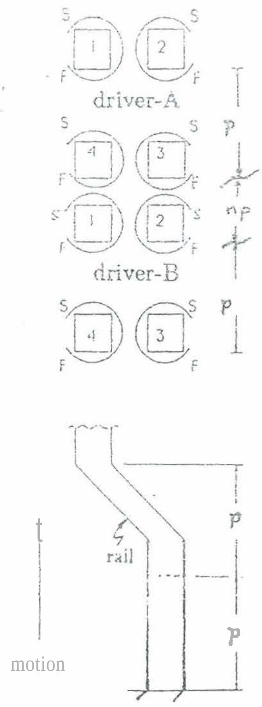

Fig.4 Trapizoidal rail

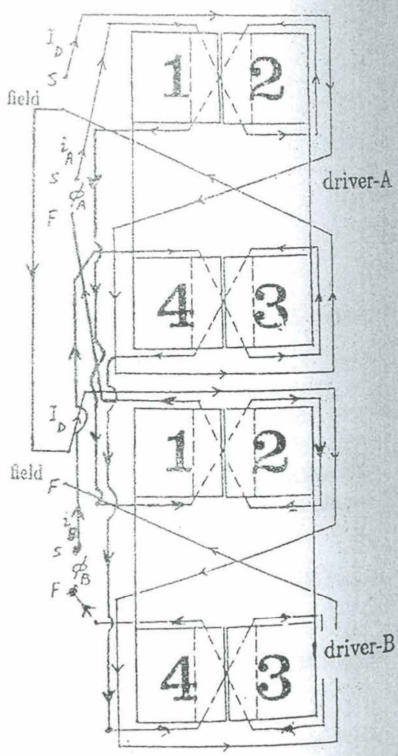

Fig.5 Coil connections for TRSM drivers

AE

ZHAR ENGINEERING THIRD
ERNATIONAL CONFERENCE
EMBER 18-21, 1993

THRUST DERATING DUE TO S

TRAPIZOIDAL LINEAR SYNCHR

LIFT AND THRUST

S. M

* Assistant prof., Electr
Umm-Ul-Qura University, P

ABSTRACT

The Trapizoidal Linear Synchronous
magnets one of which is shown in Fig.
boggie as shown in Fig.2, and are
shown in Fig.3. The coils of each ma
dc coils fed from a chopper power a
lift at constant gap, Z. The feedbac
proportional to gap position and spe
the other hand, fed from a two-phas
that the field is distorted among th
propulsion is obtained.

It was found necessary to make a tv
harmonic currents in the field circuits
armature mmf peak value equals to al
thrust force relative to supported wei
the pole-pitch shown in Fig.3.

The work described in the proposed
of TLSMP and proves that the abov
controllable lift system. To make it
must be severely derated to gain stab